Synaptonemal Complex Antigen Location and Conservation

Peter B. Moens,* Christa Heyting,‡ Axel J. J. Dietrich,‡ Willem van Raamsdonk,§ and Qianfa Chen*

*Department of Biology, York University, Downsview, Ontario, Canada M3J 1P3; ‡Institute of Human Genetics and §Zoological Laboratory, University of Amsterdam, The Netherlands

Abstract. The axial cores of chromosomes in the meiotic prophase nuclei of most sexually reproducing organisms play a pivotal role in the arrangement of chromatin, in the synapsis of homologous chromosomes, in the process of genetic recombination, and in the disjunction of chromosomes. We report an immunogold analysis of the axial cores and the synaptonemal complexes (SC) using two mouse monoclonal antibodies raised against isolated rat SCs. In Western blots of purified SCs, antibody II52F10 recognizes a 30- and a 33-kD peptide (Heyting, C., P. B. Moens, W. van Raamsdonk, A. J. J. Dietrich, A. C. G. Vink, and E. J. W. Redeker, 1987, *Eur. J. Cell Biol.*, 43: 148–154). In spreads of rat spermatocyte nuclei it produces gold grains over the cores of autosomal and sex chromosomes. The cores label lightly during the chromosome pairing stage (zygotene) of early meiotic prophase and they become more intensely labeled when they are parallel aligned as the lateral elements of the SC during pachytene (55 grains/μm SC). Statistical analysis of electronically recorded gold grain positions shows that the two means of the bimodal gold grain distribution coincide with the centers of the lateral elements. At diplotene, when the cores separate, the antigen is still detected along the length of the core and the enlarged ends are heavily labeled. Shadow-cast SC preparations show that recombination nodules are not labeled. The continued presence suggests that the antigens serve a continuing function in the cores, such as chromatin binding, and/or structural integrity. Antibody III15B8, which does not recognize the 30- and 33-kD peptides, produces gold grains predominantly between the lateral elements. The grain distribution is bimodal with the mean of each peak just inside the pairing face of the lateral element. The antigen is present where and while the cores of the homologous chromosomes are paired. From the location and the timing, it is assumed that the antigen recognized by III15B8 functions in chromosome pairing at meiotic prophase. The two anti-rat SC antibodies label rat and mouse SCs but not rabbit or dog SCs. A positive control using human CREST (calcinosis, Raynaud's phenomenon, esophageal dysmotility, sclerodactyly, telangiectasia) anti-centromere serum gives equivalent labeling of SC centromeres in the rat, mouse, rabbit, and dog. It is concluded that the SC antigens recognized by II52F10 and III15B8 are not widely conserved. The two antibodies do not bind to cellular or nuclear components of somatic cells. In these respects, the antibodies raised against isolated SCs differ from autoimmune sera and naturally occurring antibodies with anti-SC activity, which are directed against conserved epitopes shared by several cellular components (Dresser, M. E., 1987, *In* Meiosis, Academic Press, Inc., New York, 245–274).

THE meiosis-specific events of homologous chromosome pairing, genetic recombination, and chromosome disjunction are, with few exceptions, mediated by the unique organelle of the meiotic prophase nucleus, the synaptonemal complex (SC)[1] (Fig. 1) (Moses, 1958; Gillies, 1984; von Wettstein et al., 1984). In protists, fungi, plants, and animals alike, the SC consists of two parallel-aligned chromosome cores (Fig. 1, *a*, *b*, and *c*) with laterally extended chromatin loops (Fig. 1 *a*) (Weith and Traut, 1980; Rattner et al., 1981). Inferences about SC functions generally come from electron microscope observations of SCs of organisms with conventional or with exceptional meiosis. It is expected that the SC functions can be analyzed experimentally when SC components have been identified. So far, however, proteins isolated from meiotic nuclei (Meistrich and Brock, 1987) and meiosis-specific transcripts (Magee, 1987) have failed to identify SC components. Heyting et al. (1985, 1987) developed a procedure for the isolation of SCs in quantities sufficient for biochemical and immunocytochemical analysis. In one- and two-dimensional gels, several polypeptides copurify with SCs, particularly a 30- and a 33-kD polypeptide. The presence of these and other peptides in the SC is under investigation. Immunocytochemistry of spermato-

1. *Abbreviations used in this paper*: CREST, calcinosis, Raynaud's phenomenon, esophageal dysmotility, sclerodactyly, and telangiectasia; LE, lateral element; SC, synaptonemal complex.

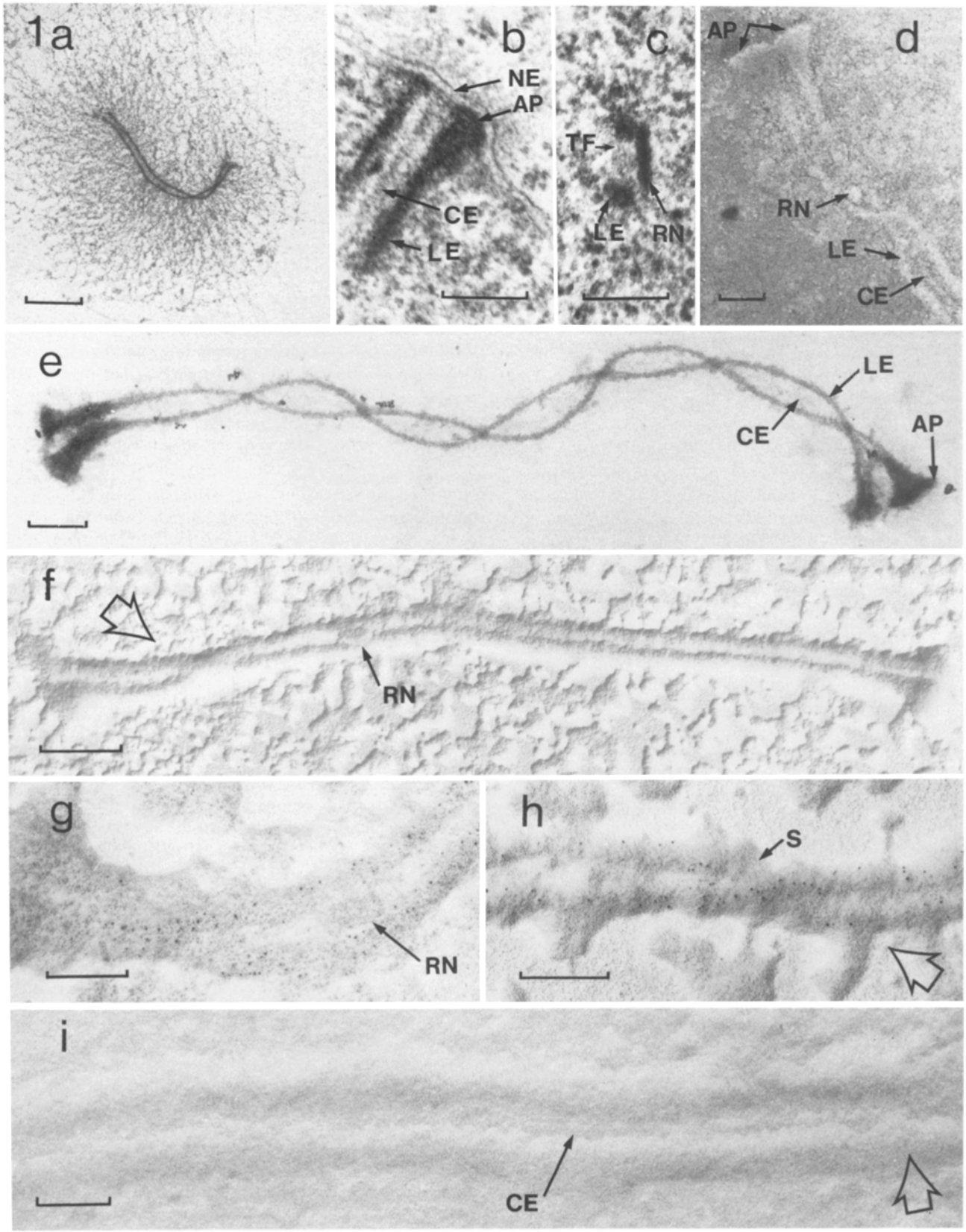

Figure 1. Comparisons of synaptonemal complex substructures visualized by surface spreading, sectioning, negative staining, isolation procedures, shadow casting, and immunogold labeling. (*a*) A surface-spread moth SC (*Hyalophora columbia*) illustrating the arrangement of the chromatin relative to lateral elements of the SC. The attachment of chromatin loops to the lateral element (Weith and Traut, 1980) is referred to as the chromatin-binding function of the LE in this paper. (*b*) Section of a rat spermatocyte nucleus to illustrate the SC attachment (*AP*) to the nuclear envelope (*NE*). CE, central element; LE, lateral element. (*c*) A recombination nodule (*RN*) on one side of a cross section of a SC with lateral elements (*LE*) and transverse filaments (*TF*). Recombination nodules (*RN*) in such an asymmetric position

cytes has yielded several antibodies with anti-SC activity (Moses et al., 1984; Dresser, 1987) and specific anti-SC monoclonal antibodies (Heyting et al., 1987). With these antibodies, aspects of core synthesis, SC formation, composition, modification, function, and conservation may be probed. In this paper we report an immunogold analysis of core and SC-specific antigens as they are detected by two monoclonal antibodies raised against isolated rat SCs.

To determine the exact position of antigens within the confines of the 120-nm-wide SC, accurate and cumulative measurements are required. Thin sections of spermatocyte nuclei (Fig. 1, *a–c*) are not well suited to the immunogold detection of SC antigens: only short fragments of SCs are visible, fixation tends to interfere with antigenicity (Eldred et al., 1983), cryosections are difficult to collect in large numbers, and colloidal gold-labeled secondary antibody penetrates poorly into sections (Slot and Geuze, 1983). Large-scale analysis is possible in surface-spread spermatocytes (Counce and Meyer, 1973; Dresser and Moses, 1980). The immunogold labeling of spreads developed by M. Dresser (National Institute of Environmental Health Sciences, Research Triangle Park, NC; personal communication) is described here as well as modifications that improve accessibility and the level of labeling. A sensitive method for the measurement and statistical analysis of gold grain distribution along the SC was developed to yield distributional profiles for the monoclonal antibodies. The profiles allow accurate comparisons between antigen locations for these and other SC antibodies.

Materials and Methods

Antibodies

Anti-SC mAbs II52F10 and III15B8 were obtained from BALB/c mice injected with purified Wistar rat SCs (Heyting et al., 1985, 1987). Isolated SCs (Fig. 1 *e*) consist of lateral elements, a central element, the enlarged SC ends, and the attachment plaques. Clones were screened for antibodies against these SC components. The culture medium of clone II52F10 contained 13 μg/ml of IgG and the medium of clone III15B8 contained 27 μg/ml of IgG. The antibodies were detected by positive diaminobenzidine staining of SCs in spread rat spermatocytes treated with antibody and rabbit anti-mouse peroxidase successively. A control mAb against a 52-kD antigen from fish brain homogenate (37B5; 10 mg IgG/ml) did not give positive indirect immunoperoxidase staining of SCs (Heyting et al., 1987). Anticentromere (kinetochore) serum was obtained from a patient with the CREST (calcinosis, Raynaud's phenomenon, esophageal dysmotility, sclerodactyly, telangiectasia) syndrome of scleroderma (Brenner et al., 1981; Earnshaw et al., 1984). Anticentromere activity of the serum was verified on cultured Chinese hamster ovary (CHO) cells and spermatocytes. Spermatocytes were obtained from BALB/c mice, Wistar rats, one rabbit, one dog (veterinary surgery), two pigeons, and a grasshopper (*Chloealtis conspersa*). The spread in Fig. 1 *a* was obtained from the moth, *Hyalophora columbia*. The activity of the mAbs and the CREST serum on somatic cells was tested with immunofluorescence of hepatocytes, human epithelial cells (HSp-2; Daymar Laboratories, Inc., Toronto, Ontario), CHO cells (D442-1), and primary rat fibroblasts (FSD2c).

Immune Staining

For electron microscope analysis of antigen location and conservation, spermatocytes were surface spread (Counce and Meyer, 1973; Dresser and Moses, 1980), picked up on plastic-coated slides, and fixed in 4% paraformaldehyde (pH 8.2 with 0.1% SDS) for 3 min and in 4% paraformaldehyde without SDS for an additional 3 min. After a 10-s rinse in 0.4% Photoflo (pH 8, Kodak Laboratory and Speciality Chemicals, Eastman Kodak Co., Rochester, NY) the slides were dried. Usually treatment continued after 30 min but slides could be stored at −20°C for 2 wk without much loss of antigenicity. After fixation cells were washed in PBS pH 7.4 and treated with DNase I (type II No. D4527; Sigma Chemical Co., St. Louis, MO), 1 μg/ml in MEM (No. 320.1570; GIBCO, Grand Island, NY), at room temperature for 30 min. Slides were washed in PBS and accumulated in holding buffer (1:20 antibody dilution buffer in PBS). Slides were incubated for 30 min at room temperature with antibody in antibody dilution buffer (3% BSA, 0.05% Triton X-100 in PBS; M. E. Dresser, personal communication). Monoclonal II52F10 was diluted 1:10 or 1:40, III15B8 was used 1:1, and CREST serum was diluted 1:40. Controls were incubated in goat serum without primary antibody. After washes in PBS, slides were incubated with secondary antibody conjugated with either 5 nm colloidal gold (Janssen Pharmaceuticals, Beerse, Belgium), with FITC, or with peroxidase (Daymar Laboratories, Inc.). For EM, gold-stained material was washed, dried well, then treated with 0.1% OsO_4 in water or in cacodylate buffer pH 7.4 for 30 min. After washes and a rinse in Photoflo, the slides were dried. The plastic film with cells was floated off and 100-mesh grids were placed on the floating film. Film and grids were picked up with Parafilm and dried. The peroxidase-conjugated material was treated as described by Heyting et al. (1987) with a 60-min exposure to DAB plus H_2O_2 for light microscopy or a 5-min exposure followed by a 30-min incubation in 0.1% OsO_4 for electron microscopy.

Quantification of Immunogold Distribution

The positions of individual gold grains relative to the LEs of OsO_4-stained and unstained SCs were recorded from magnified electron micrographs (163,000×; 5-nm gold = 0.8 mm) with a digitizer (Numonics Corp., Landsdale, PA) (±0.5 mm) and stored on computer discs. For each grain, the digitizer was set to 0 for the outer edge of the left LE (Fig. 2, point A) and then, perpendicular to the SC, coordinates of points B, D, E, and P were entered. Each file contained the measured grain positions of a given SC. No measurements were made where the SC was twisted, where the LEs were indistinct, or near the ends. A computational program accessed the stored data and calculated the widths of the LEs at the position of each gold grain (Fig. 2, A–B, D–E, and *a*), the centers of the LEs (Fig. 2, F and G), and the center of the SC (C) as ½ the distance from F to G (b). The distance of gold grain P to the nearest LE center is c. Its position in terms of the LE width was $f = c/0.5a$ and its adjusted position was $f \times 20$ nm for standardized 40-nm-wide LEs. The average distance (b) from the center of the SC (C) to the center of the LE (G) was 60 nm. The sums and sums of the squares were accumulated for parameters *a*, *b*, *c*, and $f \times 20$ nm. From these, the means, standard deviations, and standard errors of the means were calculated. Files for a given treatment were combined to compare the labeling pattern between antibodies and between animals (Fig. 3). The histograms were based on totals of 697 grains for II52F10 on rat SCs, 707 grains

---

are also visible in negative-stained and shadow-cast preparations (*d*, *f*, and *g*). (*d*) A negative-stained surface-spread SC. Elevated structures are electron transparent. It is expected that superficial immunogold staining (Slot and Geuze, 1983) will detect antigens in the exposed structures. (*e*) Isolated SCs used to inoculate mice (Heyting et al., 1985, 1987) consist of lateral elements (*LE*), a central element (*CE*), transverse filaments connecting the two, attachment plaques (*AP*), and the enlarged SC ends at late pachytene and diplotene. Hybridoma clones were screened for antibodies against those SC components. (*f*) Directional shadow cast of a mAb II52F10 immunogold-stained SC to illustrate the exposed SC components that include the enlarged ends, lateral elements, a twist, and a recombination nodule (*RN*). The open arrow marks the direction of the platinum–gold application (angle 7°). (*g*) Rotary shadow cast of a mAb II52F10 immunogold-stained SC demonstrates the absence of gold grains over the recombination nodule (*RN*). (*h*) Directional shadow-cast, II52F10 immunogold-stained SC demonstrates that at a twist only the upper lateral element is labeled. There are no grains in the shadowed lower LE. The observation confirms that immunogold staining is superficial. Open arrow points to the direction of shadow casting. (*S*) Shadow. (*i*) A fine-textured shadow-cast SC preparation demonstrates the exposed central element (*CE*). Bars: (*a*) 1 μm; (*b–e*, *g–i*) 0.2 μm; (*f*) 0.5 μm.

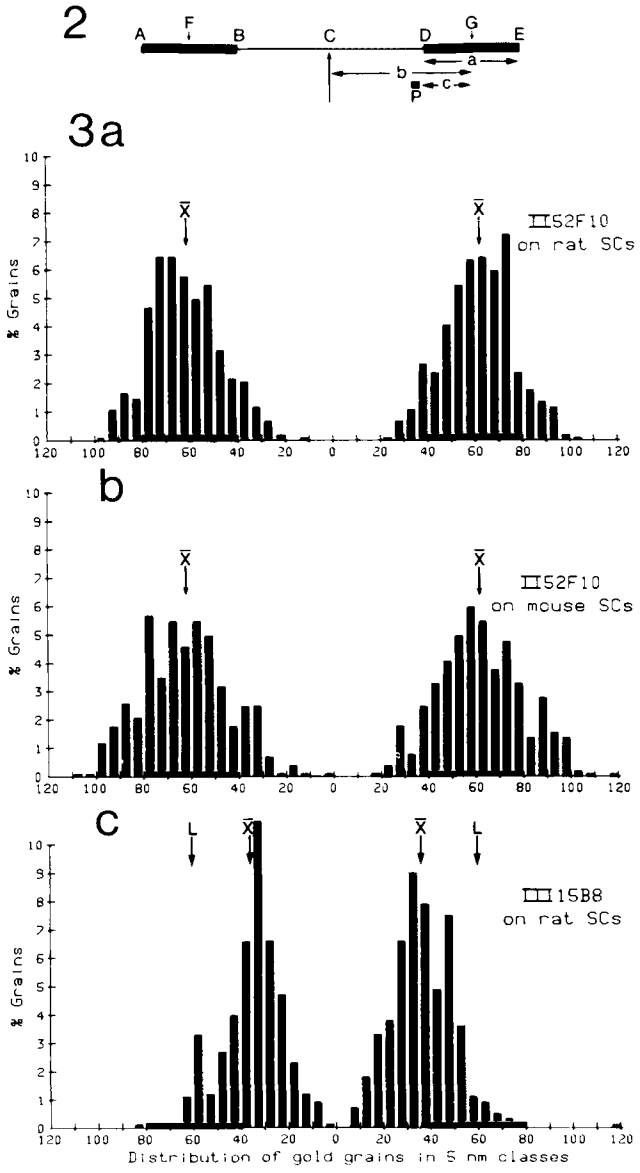

Figures 2 and 3. (Fig. 2) A diagrammatic cross section of an SC to illustrate the procedure for measuring gold grain positions in unstained and OsO_4-stained preparations. Lateral elements A–B and D–E with centers F and G. The SC center is C, the width of the LE is a, the distance from the SC center to LE center is b, and the distance from the gold grain P to the nearest LE center is c. (Fig. 3) Histograms of accumulated gold grain distributions over cross-sectional SC profiles. The horizontal bars mark the LEs that are 40-nm wide and at a distance of 40 nm from the SC center at 0. The $\bar{X}$s mark the means of gold grain distributions and L the center of the LE. (*a*) The distribution of 697 gold grains on rat SCs treated with mAb II52F10. The means, $\bar{X}$, are close to the LE centers (2 and 1 nm to the outside). (*b*) The distribution of 707 gold grains on mouse SCs treated with mAb II52F10. The means, $\bar{X}$, are 2 nm to the outside of the LE centers. (*c*) Distribution of 544 gold grains on rat SCs treated with mAb III15B8. The means, $\bar{X}$, are 26 and 23 nm to the inside of the LE centers (L).

for II52F10 on mouse SCs, and 544 grains for III15B8 on rat SCs. There was no real distinction between left and right LE since the two alternate at every twist in the SC. The numbers of SCs available from each treatment were essentially unlimited and the numbers of SCs analyzed were restricted only by practical considerations.

Results

Immune Staining Controls

The lack of aspecific mouse IgG binding to rat meiotic chromosome cores and synaptonemal complexes was demonstrated previously (Heyting et al., 1987) by the use of mouse IgG mAb 37B5 against a 52-kD peptide from fish brain homogenate. Aspecific binding of gold conjugated goat IgG against mouse IgG was found to be negative in the SCs of spread spermatocyte preparations treated with holding buffer instead of the primary mouse mAb II52F10 or mAb III15B8. The general availability of antigenic sites in rabbit and dog SCs, where the mAbs were negative, was confirmed by the immunogold staining of SC centromeres with CREST serum. Since the three antibodies, II52F10, III15B8, and CREST, stain different parts of the same structure, they furthermore serve as positive controls to each other.

SC Topography

Surface spreading of spermatocytes, combined with immunogold staining, promotes the detection of exposed surface antigens. The SC surface topography was visualized with negative staining (Fig. 1 *d*) and shadow casting of spread SCs (Fig. 1, *f–i*, and Fig. 6 *a*). In negatively stained preparations, the elevated contours are electron transparent and include attachment plaques, a recombination nodule, the LE, and CE. Directional shadow casting shows that the LEs are raised above the background and that the recombination nodule is positioned on top of the LEs (see cross sectioned SC in Fig. 1 *c*). The central element is also evident at the surface of the SC in the fine-textured shadow-cast image in Fig. 1 *i*. Directional shadow casting of II52F10 immunogold-labeled LEs shows that at the twists, where one LE passes over the other, only the upper LE is labeled (Fig. 1 *h*). It is concluded that, in general, the SC antigens that are exposed at the surface of the preparation are stained by the immunogold procedure.

mAb II52F10 on Rat SCs

The distribution of gold grains over rat SCs is shown in low magnification in Fig. 4 *a* and in detail in Fig. 4 *b*. The gold grains are located predominantly over the LEs, while the central element has proportionally few grains. In general, centromeric regions are free from grains except where one of the lateral elements is brought to the surface of the spread cell by a twist in the SC. In shadow-cast preparations of gold-labeled SCs (Fig. 1 *h*), it is evident that only the upper LE of a twist has the grains.

The distribution of 697 grains from the analyzable portions of five SCs is shown in the histogram of Fig. 3 *a*. The diagrammatic cross section of a SC in Fig. 2 and the horizontal bars in Fig. 3 compare the distribution of gold grains in the histogram to the structure of the SC. The lateral elements (Fig. 2) A–B and D–E are, on average, 42-nm wide but they are standardized to 40 nm in the histogram. 80% of the grains are located over the LEs, 10% lie in the medial region of the SC, and 10% lie to the outside of the LEs. Since the value 20 nm × $c/0.5a$ is used to calculate the position of each grain in the histogram, their locations relative to the LEs are automatically adjusted for SCs wider or narrower than the average. The mean of grain positions, $\bar{X}$, for each peak is

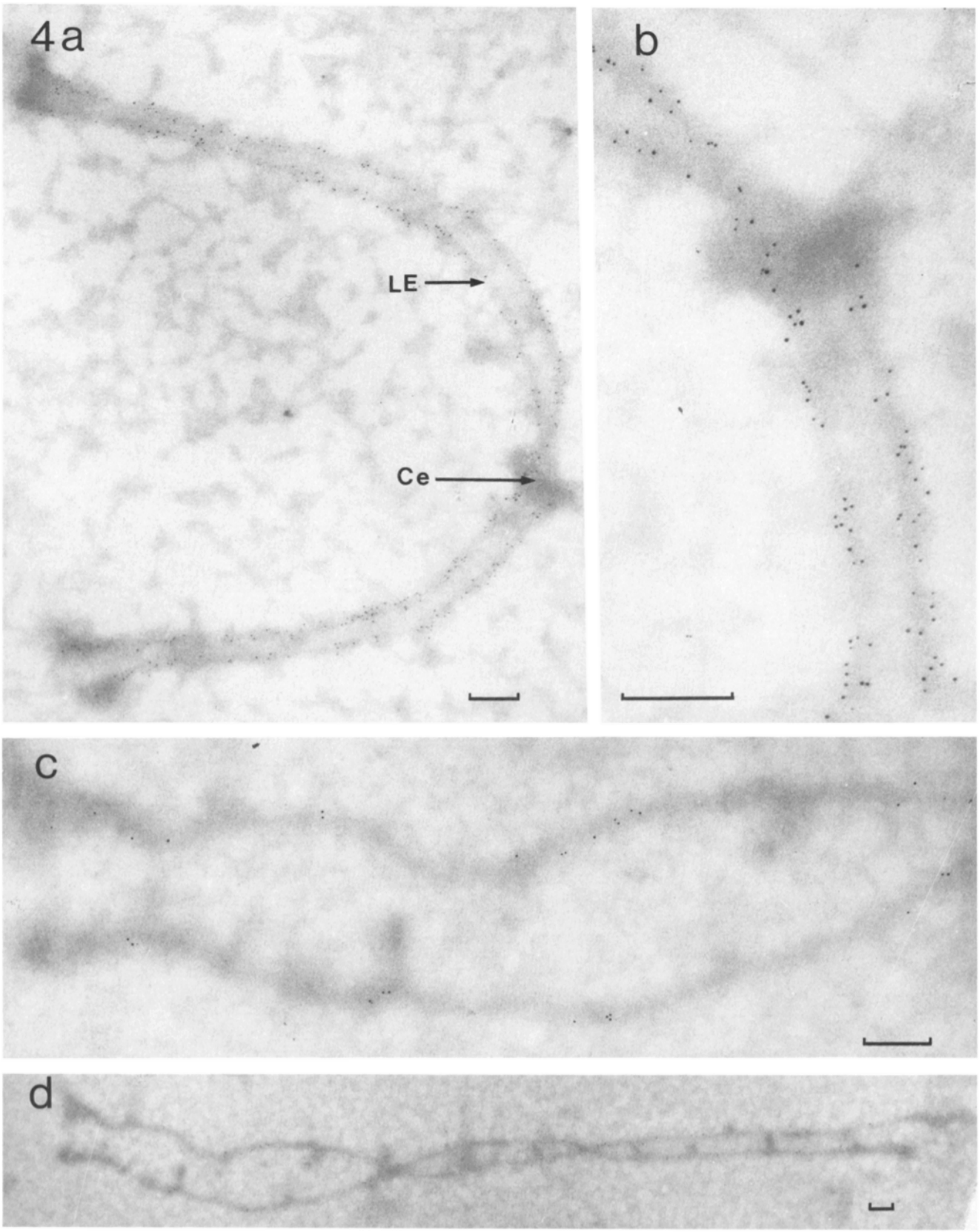

Figure 4. mAb II52F10 on rat SCs. (*a*) A complete SC with a medially located centromere (*Ce*). The 5 nm gold grains are predominantly on the lateral elements (LE). Background staining is negligible. (*b*) The centromeric region normally has no grains. In this case the SC twist has brought the upper lateral element to the surface where it is accessible to the gold-labeled secondary antibody. (*c*) The chromosome cores are already lightly labeled before they pair during the zygotene stage of meiotic prophase. The stage is easily differentiated from the later diplotene stage when the cores have heavily labeled enlarged ends (Fig. 5, *d* and *e*). (*d*) A lower magnification of *c* illustrating the entire SC in the process of synapsis. Bars, 0.2 μm.

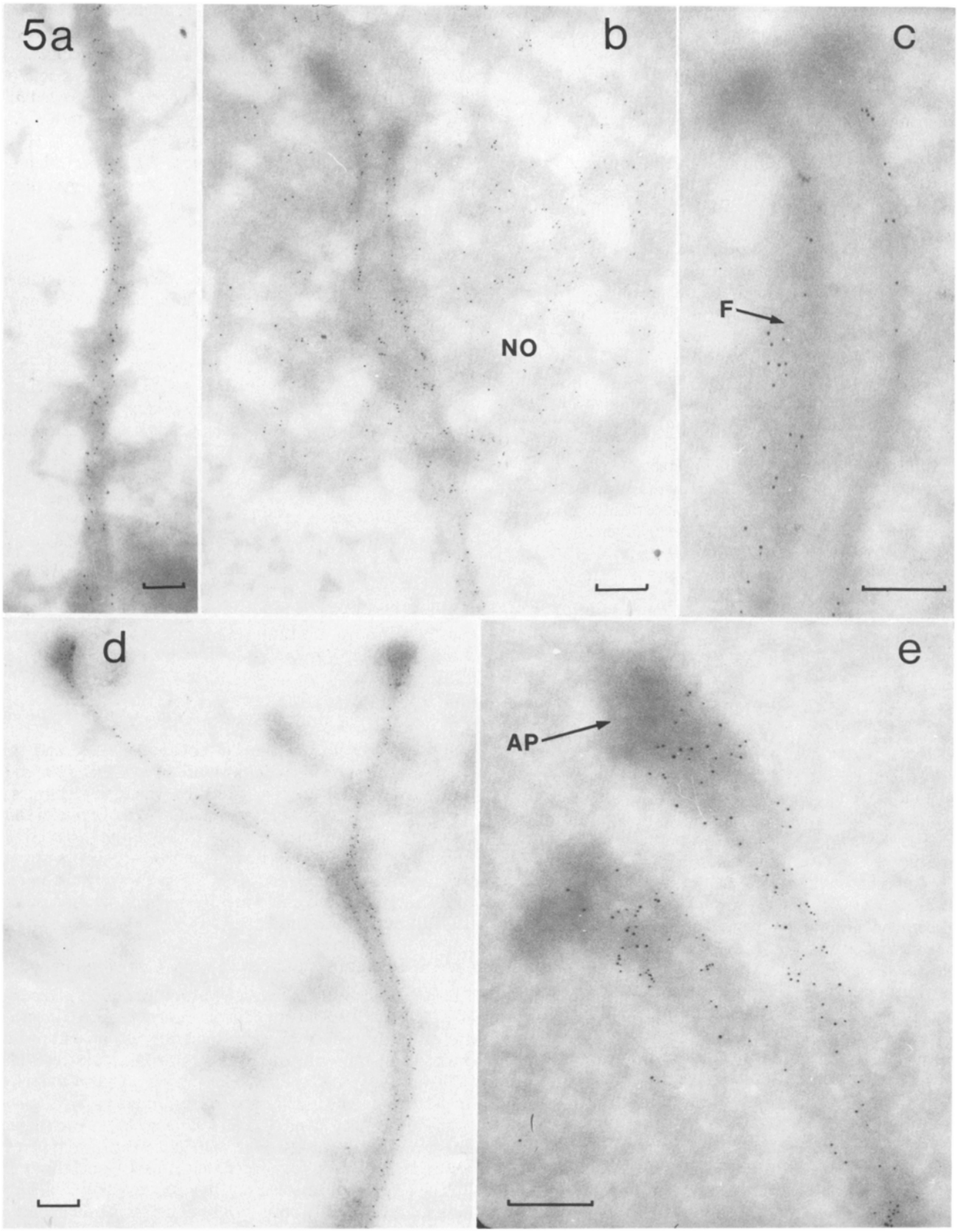

Figure 5. Additional mAb II52F10 labeling patterns. (*a*) Segment of an unpaired X chromosome core. The entire core and the Y chromosome core are labeled at the same or greater density than the autosomal SC lateral elements at pachytene. (*b*) Distribution of label in the nucleolus (*NO*). (*c*) Distribution of label in a swollen lateral element (*F*). These subterminal enlargements are found in occasional early pachytene nuclei and have been reported in mammals, insects, and plants. (*d*) The antigen is still present in the chromosome cores when they start to disjoin at the onset of diplotene. (*e*) Distribution of label on the enlarged terminal SC segments. The extreme ends (*AP*) have few grains. Bars, 0.2 μm.

within 2 nm of the LE center. The average density along the length of the SC is 55 grains per micrometer of SC length (1,934 grains over 34.9 μm SC).

The antigen recognized by mAb II52F10 is detected on the chromosome cores when they first form and pair during the zygotene stage of meiotic prophase (Fig. 4, *c* and *d*). The level of labeling is low at this early stage and, unlike the late stages, the ends do not have large numbers of grains. The dense bars between the lateral elements do not contain the antigen (Fig. 4, *c* and *d*). The structure, numbers, and time of occurrence of the bars indicate that these are not recombination nodules (Moens, 1978). Recombination nodules equivalent to those analyzed in sectioned rat spermatocytes (Fig. 1 *c*) were observed on directionally shadow-cast SCs (Fig. 1 *f*) and rotary shadow-cast SCs (Fig. 1 *g*) of mAb II52F10 immunogold-stained preparations. The recombination nodule (Fig. 1 *g*) has no grains whereas the LEs to either side are well labeled. At early pachytene the cores of the X and Y chromosomes are still unpaired (Joseph and Chandley, 1984) but abundantly labeled (Fig. 5 *a*). At the same time the nucleolus is still attached to the SCs of chromosomes with a nucleolar organizer (Fig. 5 *b*). Portions of the nucleolus are gold labeled after treatment with antibody II52F10 (Fig. 5 *b*). Also at early pachytene occasional nuclei have one or more locally swollen LEs. These enlargements are labeled at the level of normal LEs (*F* in Fig. 5 *c*).

The antigen is still evident in the cores when they separate at the onset of diplotene (Fig. 5 *d*). At that time the enlarged terminal segments of the cores are heavily labeled (Fig. 5 *e*). The extreme ends (*AP*), however, have few grains. In the negative controls where holding buffer or goat serum was used instead of primary antibody, no immune staining of cores, SCs, or nucleoli was observed.

mAb II52F10 on Mouse SCs

The distribution of gold grains on mouse SCs is similar to that found on rat SCs but there are at best only some 20 grains per micrometer of SC length (480 grains on 24.5 μm of SC) as compared with 55 grains per micrometer of SC length in the rat. The distribution of 707 grains in 5-nm classes across the width of the SC is illustrated in the histogram (Fig. 3 *b*). The average width of the LEs is 38 nm but has been standardized to 40 nm. The means of the bimodal grain distribution, $\bar{X}$, are within 3 nm of the LE centers. 71% of the grains are located over the LEs, 12% between the LEs, and 17% to the outside. The means of the gold grain positions are not significantly different in mouse and rat ($t = -0.0340$, $t_{0.05(2)\infty} = 1.962$). As in the rat, cores are labeled from zygotene through pachytene into the onset of diplotene. The X and Y chromosome cores are labeled.

Monoclonal III15B8 on Rat SCs

By inspection (Fig. 6, *a–c*) it is clear that the grains are predominantly between the lateral elements. Statistical analysis of measurements on 544 grains shows that the grains are not evenly distributed over the median region. There are two peaks and their means, $\bar{X}$ (Fig. 3 *c*), lie to the inside of the pairing face of the LE, 5.6 and 3.2 nm, respectively. Thus the means are about 24 nm to the insides of the LE centers while the means for II52F10 coincide with the LE centers. 67% of the grains lie between the LEs, 32% on the LEs, and 1% to the outside. There are only 4 grains/1 μm of SC as compared with 55 for mAb II52F10, even though the IgG content of clone III55B8 supernatant is twice that of II52F10, and III15B8 supernatant is used in a 1:1 dilution compared with 1:40 for II52F10. The grains occur along the length of the SC while it is fully paired at pachytene (Fig. 6, *a* and *b*). When cores separate at the onset of diplotene, with few exceptions grains are only in the paired portion of the SC (Fig. 6 *c*). So far it has not been possible to determine which of the SC peptides reacts with mAb III15B8 in Western blots from one-dimensional gels of purified SCs.

mAb III15B8 on Mouse SCs

The distribution of the grains over the mouse SCs is identical to that shown for rat SCs (Fig. 3 *c*). The means of the bimodal distribution of 174 grains are also 5 nm to the inside of each LE. Grains are present only where the cores are paired. In the mouse the unpaired X chromosome frequently has pseudo-SCs along parts of its length and those segments also label with mAb III15B8. In most preparations mAb III15B8 produces fewer grains on mouse SCs than on rat SCs, but occasionally mouse SCs have similar numbers of grains as rat SCs.

mAbs II52F10 and III15B8 on SCs of Other Species

No immunogold label could be detected with either mAb II52F10 or III15B8 on the SCs of a rabbit, dog, pigeon, or grasshopper. The human CREST anticentromere serum stains the centromeres of rat, mouse, rabbit, and dog SCs equally well under the same staining protocol (Fig. 6, *d* and *e*). The pigeon and grasshopper SCs were not tested with the CREST serum.

SC Specificity of mAbs II52F10 and III15B8

CHO cells, hepatocytes, human epithelium cells, and rat fibroblasts were tested with mAbs 52F10 and III15B8, and FITC-conjugated secondary antibody. The lack of fluorescence suggests the absence of antigenic sites in the nuclei and the cytoplasm in those cells. The CREST serum was used as a positive control in the CHO cells and the fibroblasts where it causes a bright fluorescence of nuclear components. In rat spermatocytes only the SCs and the nucleoli in the case of II52F10 show fluorescence.

CREST Immunogold Labeling of SC Centromeres

The main component of the meiotic prophase nucleus recognized by the CREST antibodies is the centromere (kinetochore). In the mouse each centromere is at one end of its chromosome. Accordingly one end of the SC fluoresces with FITC-labeled secondary antibody (Fig. 6 *e*). The rat and rabbit SCs with interstitially located centromeres have gold grains in the corresponding positions (Fig. 6 *d*). The single centromeric region consists of two juxtaposed centromeres as is apparent when the two centromeres are slightly misaligned (Fig. 6 *d*). The centromeres are also labeled before pairing. The CREST serum gives noticeable immune staining of the SCs after mild DNA digestion (Fig. 6, *d* and *e*). In this study, the CREST serum was used as a positive control to verify that antigenic sites were accessible and to check the protocol when mAbs II52F10 and III15B8 failed to stain the SCs of dog or rabbit spermatocytes, and where they failed to stain somatic cell components.

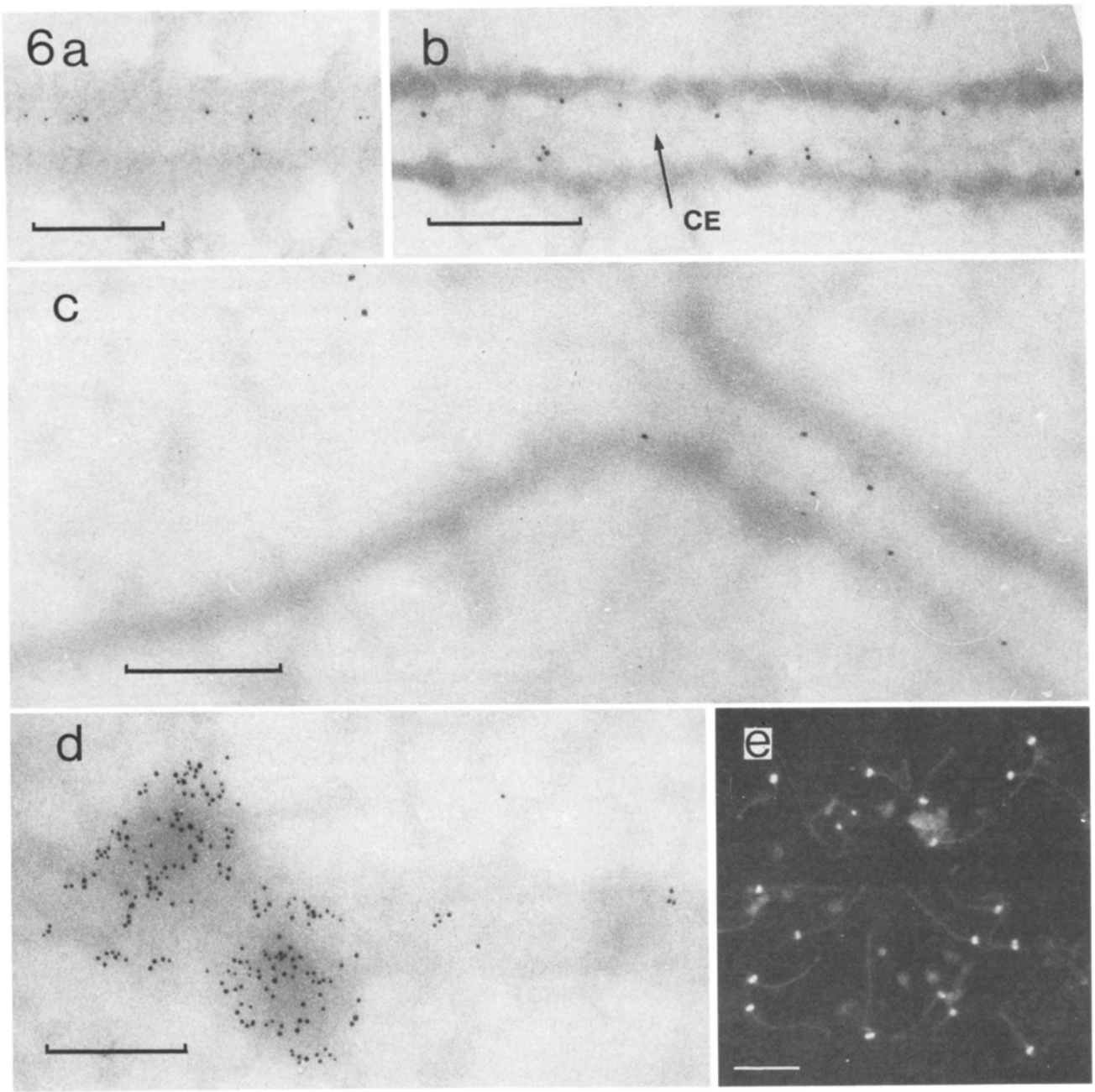

Figure 6. mAb III15B8 and CREST serum staining of SCs. (*a*) A rotary shadow-cast rat SC illustrates the location of grains on the inner edges of the lateral elements. Shadow-cast LEs appear broader than stained (*b*) or unstained (*c*) LEs. (*b*) An OsO_4-stained mouse SC demonstrates that SCs of the two species have the same distribution of label and that the grains are just to the inside of the OsO_4-stained lateral element (Fig. 3 *c*). The central element is not labeled. (*c*) An unstained mouse SC at diplotene illustrates the presence of gold grains in the paired portion of the SC. Rarely are there grains on the unpaired cores. (*d*) CREST-labeled centromeres of a rabbit SC. CREST labels the SC centromeres of all species tested but the two mAbs label only rat and mouse SCs. (*e*) CREST immunofluorescence of SC centromeres that, in the mouse, are located at one end of each SC. The SCs also fluoresce after mild DNAse digestion of the chromosomes. Various other nuclear components also show immunofluorescence. Bars: (*a–d*) 0.2 μm; (*e*) 4 μm.

Techniques

The effectiveness of SC immune staining for EM was tested with several protocols. Agar filtrates of rat spermatocytes (Dietrich and De Boer, 1983) gave excellent indirect immunoperoxidase staining in light microscopy (Heyting et al., 1987) and in EM but the localizations of antigens was not precise or quantifiable within the dimensions of the SC. The immunogold staining of SCs in agar filtrates did not yield high levels of gold labeling and the use of grids restricted the amount of material that could be processed. In surface spreads large numbers of spermatocytes could be processed together. Spread spermatocytes fixed in 4% paraformaldehyde with 0.03% SDS had excellent SCs but they were contained in nuclear substrate that appeared to reduce the accessibility of SCs for the gold-conjugated secondary antibody. Those SCs that had fallen away from the nucleus were well stained. To

improve the dispersion of SCs the SDS concentration was increased to 0.06 and 0.09%. In all animals studied, the higher concentrations gave large numbers of free SCs. Measurements were made on the shortest SCs only (4–5 μm).

Mild DNase I digestion of spread spermatocytes was found to markedly increase the immunogold staining of SCs with the monoclonal antibodies. Fixation and staining with OsO_4 improved the electron opacity of chromosome cores and LEs but the gold grains had to be immobilized by drying the slides well before OsO_4 treatment. Phosphotungstic acid stained the background more than OsO_4. To optimize washing of slides and treatments with DNase, Triton X-100, and holding buffer, all solutions were kept in constant circulation with stir bars.

Discussion

To gain an understanding of how the axial cores and the SCs accomplish their several functions in chromatin arrangement, chromosome pairing, recombination, and disjunction at meiosis it is necessary to know the components that combine to form the SCs (Ierardi et al., 1983; Heyting et al., 1985, 1987). Antibodies directed against SC components provide a first approach to the identification of SC substructures and their functions. In this report we describe the structural, temporal, and phylogenetic distribution of antigens detected by two mouse monoclonal antibodies raised against isolated rat SCs and we consider the functional properties of the antigens.

In Western blots of purified SCs, the peptides recognized by mAb II52F10 have molecular masses of 30 and 33 kD (Heyting et al., 1987). The purified SCs come from spermatocytes in a range of meiotic prophase stages and the quantitative relation between the two peptides at different stages is obscured. One or both may be present at consecutive stages and they may or may not be evenly distributed. The changes in the observed labeling pattern from pachytene to diplotene (Figs. 4 and 5) may be due to *de novo* exposure of one or the other peptide, or to a redistribution of peptides, or to a modification of existing peptides. The consistent localization of mAb II52F10 to the chromosome core suggests that the 30- and 33-kD peptides are closely related and that the one may be a modified form of the other. Since immunogold staining tends to detect antigens at the surface of the preparation (Fig. 1 *h*) (Slot and Geuze, 1983), it can only be ascertained that the peptides detected by II52F10 are on the surface of the LE. Their presence in the interior of the core cannot be determined in spread preparation. The immunogold is predominantly over the LE (80%, Figs. 3 *a* and 4) and evenly present along the length of the LE (Figs. 4 *a* and 5 *a*) with the exception of the terminal segment of the enlarged SC ends at late pachytene and diplotene (Fig. 5, *d* and *e*). In sectioned material this terminal segment corresponds to the dense-staining attachment plaque of the SC to the nuclear envelope (Fig. 1 *b*), and to the light area in the negatively stained SC in Fig. 1 *d*. The attachment plaque is immunogold labeled by SC3, a mAb from an autoimmune mouse with activity against cytoplasmic intermediate filament-like material, SC attachment plaques, and the central element (Moses et al., 1984). Thus it appears that the antigens recognized by SC3 and II52F10 have mutually exclusive compartments in the SC. By inference they have different functions.

The continued presence of the peptides recognized by 52F10 on the chromosome core from the time when the cores first form until they disappear suggests that the antigens have a continuing function. These antigens, therefore, are not likely involved in the temporary SC functions such as pairing, recombination, or disjunction. The absence of grains over the central element and over the recombination nodules (Fig. 1 *g*; Carpenter, 1984) further argues against a role of the antigens in the process of pairing or recombination. A more continuous function of the SC, such as chromatin-binding function or a role in the structural integrity of the core, is more likely.

The antigens detected by III15B8 are distributed differently in space and time from those detected by II52F10. In unstained and OsO_4-stained preparations, the majority of the grains lies between the LEs (67%) and is predominantly present while and where the LEs are paired (Fig. 6, *b* and *c*). The grains are not evenly distributed across the medial region of the SC. There is a bimodal distribution with means at the inner edges of the LEs (Fig. 3 *c*). The central element is relatively free from grains (Figs. 3 *c* and 6 *b*). This probably reflects a real lack of antigen in that region since the central element is well exposed (Fig. 1, *d* and *i*) and stains with mAb SC3 (Moses et al., 1984; Dresser, 1987). In rotary shadow-cast SC preparations (Fig. 6 *a*), the LEs seem broader and the grains lie on the inner edges of the LEs. This suggests that the main concentration of antigens is on or near the inner edges of the LEs.

The presence of antigens recognized by mAb III15B8 between paired LEs suggests a function of the antigens in chromosome pairing. Filaments have been shown to extend between cores in the process of synapsis and the filaments then remain between the LEs as transverse filaments (Fig. 1 *c*; Moens, 1969). Since no other structures are evident in this region of the SC, it is provisionally assumed that the epitope is at the base of the transverse filament or in material that connects the transverse filament to the LE. The unpaired X chromosome core of the mouse frequently forms stretches of pseudo-SCs (Solari, 1970). These pseudo-SCs also have immunogold labeling and it is concluded that the chromosome pairing as such is not a necesssary requirement for the presence of the antigen.

The broad functional and structural similarities of SCs in a wide range of species leads to the expectation that immunocytochemical techniques will detect conserved antigenic components in the SC substructure. A number of naturally occurring antibodies with anti-SC activity and autoimmune sera with anti-SC activity appear to detect such conserved components. SC-binding antibodies are common in the sera of normal humans, mice, and rabbits (Dresser, 1987). The anti-SC activity in mice and rats of rabbit serum raised against chicken gizzard myosin (De Martino et al., 1980) may be attributable to the presence of such naturally occurring antibodies in the preimmune serum rather than to the presence of myosin in the SC (Spyropoulos and Moens, 1984). In the case of an anti-tubulin serum with anti-SC activity, affinity purification against pig brain tubulin yielded a fraction that no longer labeled SCs and a remainder of nonspecific antibodies that label SCs (Dresser, 1987). Anti-SC activity has been reported in some sera from humans

with the autoimmune CREST syndrome, for a monoclonal antibody of an autoimmune mouse, and for a monoclonal antibody from a mouse immunized with whole testis (Dresser, 1987). In these cases the sera cross-react with other proteins and the anti-SC activity extends to SCs of several mammalian species. The anti-SC activity probably involves binding to SC proteins that share an epitope with conserved proteins such as actin, vimentin, or others from which the SC proteins are otherwise distinct (Dresser and Moses 1983; Moses et al., 1984; Dresser, 1987).

Structural and functional differences between the SCs of phylogenetically related species (Zickler, 1973; Bernelot-Moens and Moens, 1986) can be expected to be associated with species-specific antigenic SC differences. The results reported here indicate that the two mAbs raised against isolated rat SCs are SC specific but that the antigens are not extensively conserved. Neither of the mAbs reacts with cytoplasmic or nuclear components of CHO cells, human epithelial cells, hepatocytes, or rat fibroblasts. Gold grains associated with III15B8 are located on the SCs only and on no other part of the spermatocyte nucleus or cytoplasm. II52F10 binds to the meiotic chromosome cores and parts of the nucleolus. The nucleolar antigenic sites need not be in conflict with the anti-SC specificity of II52F10 since SC material has been reported in meiocyte nucleoli of numerous organisms (Sotelo and Wettstein, 1964; Schrantz, 1970; Rasmussen, 1973, 1975; Moens and Rapport, 1971; Haskins et al., 1971). The antibodies raised against isolated rat SCs react with rat and mouse SCs but not with rabbit, dog, or pigeon SCs. The antigens recognized by the two mAbs are therefore not widely conserved. In addition, the antigen recognized by II52F10 has a reduced antigenicity in the mouse (35% of the rat) and it therefore is species specific.

Where the antibodies are raised against isolated SCs, the immune reaction is expected to be directed against SC proteins or epitopes that are different from "self". To what extent the male mouse recognizes SC proteins as self is uncertain, considering that SCs are formed after immune competence is achieved and that the spermatocytes lie outside the blood-testis barrier (Dym and Fawcett, 1970). If SCs are foreign, antibodies may be raised against conserved as well as species-specific elements of the SC. But even if the spermatocytes are foreign, not all of the SC proteins are necessarily foreign as they share components with such ubiquitous structures as intermediate filaments (Dresser, 1987), nuclear pores, and the nuclear envelope (Fiil and Moens, 1973).

The Institute of Human Genetics, University of Amsterdam, The Netherlands, generously provided laboratory and electron microscopy facilities for P. B. Moens while on sabbatical leave. We gratefully acknowledge assistance by Agnes C. G. Vink, Egbert J. W. Redeker, Mary Lou Ashton, and Barbara Spyropoulos. Peter Lee of Wellesley Hospital, (Toronto, Canada) provided the CREST serum. Valuable ideas and practical help with the immune staining of SCs were given by Michael Dresser (National Institute of Environmental Health Sciences, Research Triangle Park, NC) Jan-Willem Slot (Laboratory voor Electronenmicroscopie, University of Utrecht, The Netherlands), and Ruud Buys (Netherlands Institute for Brain Research, Amsterdam Medical Centre).

Received for publication 25 October 1986, and in revised form 13 March 1987.

References

Bernelot-Moens, C., and P. B. Moens. 1986. Recombination nodules and chiasma localization in two Orthoptera. *Chromosoma (Berl.)*. 93:220–226.

Brenner, S., D. Pepper, M. W. Berns, E. Tan, and B. R. Brinkley. 1981. Kinetochore structure, duplication, and distribution in mammalian cells: an analysis by human autoantibodies from scleroderma patients. *J. Cell Biol.* 91:95–102.

Carpenter, A. T. C. 1984. Recombination nodules and the mechanism of crossing over in Drosophila. *In* Controlling Events in Meiosis. C. W. Evans and H. G. Dickinson, editors. The Company of Biologists Ltd., University of Cambridge, United Kingdom. 233–244.

Counce, S. J., and G. F. Meyer. 1973. Differentiation of the synaptonemal complex and the kinetochore in Locusta spermatocytes studied by whole mount electron microscopy. *Chromosoma (Berl.)*. 44:231–253.

De Martino, C., E. Capanna, M. R. Nicotra, and P. G. Natali. 1980. Immunochemical localization of contractile proteins in mammalian meiotic chromosomes. *Cell Tissue Res.* 213:159–178.

Dietrich, A. J. J., and P. de Boer. 1983. A sequential analysis of the development of the synaptonemal complex in spermatocytes of the mouse by electron microscopy using hydroxyurea and agar filtration. *Genetica (The Hague)*. 61:110–129.

Dresser, M. E. 1987. The synaptonemal complex and meiosis: An immunocytochemical approach. *In* Meiosis. P. B. Moens, editor. Academic Press Inc., New York. 245–274.

Dresser, M. E., and M. J. Moses. 1980. Synaptonemal complex karyotyping of the Chinese hamster (Cricetulus griseus). IX. Light and electron microscopy of synapsis and nucleolar development by silver staining. *Chromosoma (Berl.)*. 76:1–22.

Dresser, M. E., and M. J. Moses. 1983. Cytological characterization of an anti-synaptonemal complex monoclonal antibody. *J. Cell Biol.* 97:185a. (Abstr.)

Dym, M., and D. W. Fawcett. 1970. Blood-testis barrier in rat and physiological compartmentalization of seminiferous epithelium. *Biol. Reprod.* 3: 308–326.

Earnshaw, W. C., N. Halligan, C. Cooke, and N. Rothfield. 1984. The kinetochore is part of the metaphase chromosome scaffold. *J. Cell. Biol.* 98: 352–357.

Eldred, W. D., C. Zucker, H. J. Karten, and S. Yazulla. 1983. Comparison of fixation and penetration enhancement techniques for use in ultrastructural immunocytochemistry. *J. Histochem. Cytochem.* 31:285–292.

Fiil, A., and P. B. Moens. 1973. The development, structure and function of modified synaptonemal complexes in mosquito oocytes. *Chromosoma (Berl.)*. 41:37–62.

Gillies, C. B. 1984. The synaptonemal complex in higher plants. *CRC Crit. Rev. Plant Sci.* 2:81–116.

Haskins, E. F., A. A. Hinchee, and R. A. Cloney. 1971. The occurrence of synaptonemal complexes in the slime mold Echinostelium minutum de Bary. *J. Cell Biol.* 51:898–903.

Heyting, C., A. J. J. Dietrich, E. J. W. Redeker, and A. C. G. Vink. 1985. Structure and composition of synaptonemal complexes, isolated from rat spermatocytes. *Eur. J. Cell Biol.* 36:307–314.

Heyting, C., P. B. Moens, W. van Raamsdonk, A. J. J. Dietrich. A. C. G. Vink, and E. J. W. Redeker. 1987. Identification of two major components of the lateral elements of synaptonemal complexes of the rat. *Eur. J. Cell Biol.* 43:148–154.

Ierardi, L. A., S. B. Moss, and A. R. Bellvé. 1983. Synaptonemal complexes are integral components of the isolated mouse spermatocyte nuclear matrix. *J. Cell Biol.* 96:1717–1726.

Joseph, A. M., and A. C. Chandley. 1984. The morphological sequence of XY pairing in the Norway rat Rattus norvegicus. *Chromosoma (Berl.)*. 89: 381–386.

Magee, P. T. 1987. Transcription during meiosis. *In* Meiosis. P. B. Moens, editor. Academic Press Inc., New York. 355–382.

Meistrich, M. L., and W. A. Brock. 1987. Proteins of the meiotic nucleus. *In* Meiosis. P. B. Moens, editor. Academic Press Inc., New York. 333–354.

Moens, P. B. 1969. The fine structure of meiotic chromosome polarization and pairing in Locusta migratoria spermatocytes. *Chromosoma (Berl.)*. 28:1–25.

Moens, P. B. 1978. Lateral element cross connections of the synaptonemal complex and their relationship to chiasmata in rat spermatocytes. *Can. J. Genet. Cytol.* 29:567–579.

Moens, P. B., and E. Rapport. 1971. Synaptic structures in the nuclei of sporulating yeast, Saccharomyces cerevisiae (Hansen). *J. Cell Sci.* 9:665–677.

Moses, M. J. 1958. The relationship between the axial complex of meiotic prophase chromosomes and chromosome pairing in a salamander (Plethodon cinereus). *J. Biophys. Biochem. Cytol.* 4:633–638.

Moses, M. J., M. E. Dresser, and P. A. Poorman. 1984. Composition and the role of the synaptonemal complex. *In* Controlling Events in Meiosis. C. W. Evans and H. G. Dickinson, editors. The Company of Biologists Ltd., University of Cambridge, United Kingdom. 245–270.

Rasmussen, S. W. 1973. Ultrastructural studies of spermatogenesis in Drosophila melanogaster Meigen. *Z. Zellforsch. Mikrosk. Anat.* 140:125–144.

Rasmussen, S. W. 1975. Synaptonemal polycomplexes in Drosophila melanogaster. *Chromosoma (Berl.)*. 49:321–144.

Rattner, J. B., M. R. Goldsmith, and B. A. Hamkalo. 1981. Chromosome organization during male meiosis in Bombyx mori. *Chromosoma (Berl.)*. 82: 341–351.

Schrantz, J.-P. 1970. Etude cytologique, en microscopie optique et electro-

nique, de quelques Ascomycetes. I. Le noyau. *Rev. Cytol. Biol. Veg.* 33: 1–100.

Slot, J. W., and H. J. Geuze. 1983. The use of protein A-colloidal gold (PAG) complexes as immunolabels in ultra-thin frozen sections. *IBRO (Int. Brain Res. Org.) Handb. Ser. Methods Neurosci. (Immunohistochemistry).*

Solari, A. J. 1970. The spatial relationship of the X and Y chromosomes during meiotic prophase in mouse spermatocytes. *Chromosoma (Berl.).* 29:217–236.

Sotelo, J. R., and R. Wettstein. 1964. Electron microscope study on meiosis: the sex chromosome in spermatocytes, spermatids and oocytes of Gryllus argentinus. *Chromosoma (Berl.).* 15:389–415.

Spyropoulos, B., and P. B. Moens. 1984. The synaptonemal complex: does it have contractile proteins? *Can. J. Genet. Cytol.* 26:776–781.

von Wettstein, D., S. W. Rasmussen, and P. B. Holm. 1984. The synaptonemal complex in genetic segregation. *Annu. Rev. Genet.* 18:331–431.

Weith, A., and W. Traut. 1980. Synaptonemal complexes with associated chromatin in a moth Ephestia kuehniella Z. *Chromosoma (Berl.).* 78:275–291.

Zickler, D. 1973. Fine structure of chromosome pairing in ten Ascomycetes. Meiotic and premeiotic (mitotic) synaptonemal complexes. *Chromosoma (Berl.).* 40:401–416.